Harnessing Medium Entropy and Oxygen Defects in Spinel Ferrite Cathodes for Enhanced Cycling Performance in Lithium-Sulfur Batteries

Jing Zhang[a], Jin Chen[a,*], Jian Wei[a,*], Yanyi Liu[a], Yuzhao Ma[a], Xiaofeng Yang[a], Yanjun Li[a]

[a] *College of Materials Science and Engineering, Xi'an University of Architecture and Technology, Xi'an 710055, China*

ABSTRACT

The unique structure of medium entropy materials has garnered significant attention in the field of batteries. As a novel cathode material for lithium-sulfur batteries, medium-entropy spinel ferrite offers boundless possibilities to tailor charge-discharge performance. Herein, abundant oxygen vacancies were implanted into medium-entropy spinel ferrites and utilized as cathode materials for lithium-sulfur batteries to address the challenges associated with sluggish shuttle and conversion kinetics of lithium polysulfides (LiPSs) during charge-discharge processes in Li-S batteries. The synergistic effect among multiple species underscores the advantages of medium entropy features. The presence of oxygen vacancies mitigates the energy barrier associated with the decomposition reaction, thereby facilitating charge transfer kinetics and promoting LiPSs conversion. Oxygen vacancies can be readily incorporated into the medium-entropy spinel ferrite, thereby enabling the distinctive medium-entropy-driven influence of oxygen vacancies on the favorable rate capability and prolonged cycling performance of lithium-sulfur batteries. This study presents a promising approach for utilizing design defects in medium-entropy ferrites within the realm of battery applications.

Keywords: Medium entropy, Spinel ferrites, Oxygen vacancy, Lithium-sulfur battery, Defect

*Corresponding author.
E-mail: jinchen@xauat.edu.cn (J. Chen)
E-mail: weijian@xauat.edu.cn (J. Wei)

engineering

Content

S1. Experimental methods

S1.1. Fabrication of cathode material

The active material (MESO-X@S, VOs-MESO-140@S), acetylene black (Super P) conductive agent, and polyvinylidene fluoride (PVDF) binder were weighed at a ratio of 7:2:1. The uniform black slurry was formed by adding PVDF, a conductive agent, and active material to 1000 μL of N-methylpyrrolidone (NMP) solvent and stirring for 2h. The black slurry is uniformly scraped on the surface of the Al foil current collector using a scraper with a certain thickness. The Al foil was dried at 60 °C for 12 h in a vacuum drying oven before being sliced using a slicer. The pole piece is weighed and transferred to the glove box.

S1.2. Li-S cell assembly

The gasket is placed in the middle of the positive electrode shell of the button battery, placed in the positive electrode sheet, separator, adding an appropriate amount of electrolyte (40 μL), lithium sheet, and negative electrode shell. The electrolyte was composed of 1M LiTFSI, 1,3-dioxolane, 1,2-dimethoxyethane (DOL/DME, 1:1, v/v), and 2 wt.%. $LiNO_3$. Under glove box conditions (H_2O<0.01 ppm, O_2<0.01 ppm), the assembled battery is sealed with a button battery packer. The battery was taken out of the glove box and allowed to stand for 12 h. Electrochemical tests were performed on the battery.

S1.3. Formation reactions of MESO

$$CO(NH_2)_2 + H_2O \rightarrow 2NH_3 + CO_2 \quad (1)$$

$$CO_2 + H_2O \rightarrow CO3^{2-} + 2H^+ \quad (2)$$

$$NH_3 + H_2O \rightarrow NH_4^+ + OH^- \quad (3)$$

$$M^{x+} + yCO_3^{2-} + xOH^- \rightarrow M(OH)x\cdot(CO_3)_y \quad (4)$$

$$M^{2+} + CO3^{2-} \rightarrow M(CO_3) \quad (5)$$

$$M(OH)x\cdot(CO_3)_y + M(CO_3) \rightarrow M_3O_4 + H_2O + CO_2 \quad (6)$$

S2. Supporting figures

Figure S1. SEM image of MESO-160.

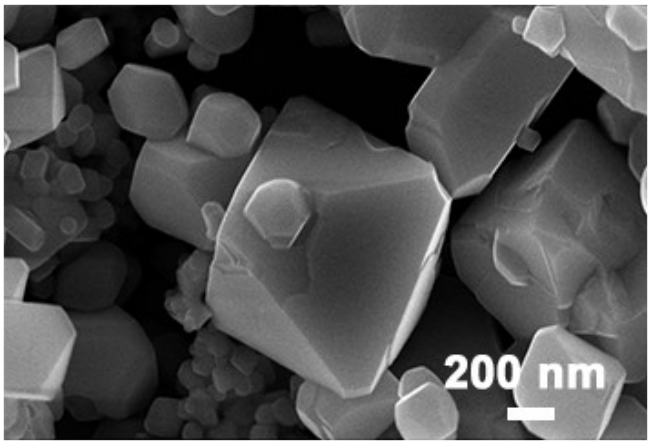

Figure S2. HRTEM image of OVs-MESO.

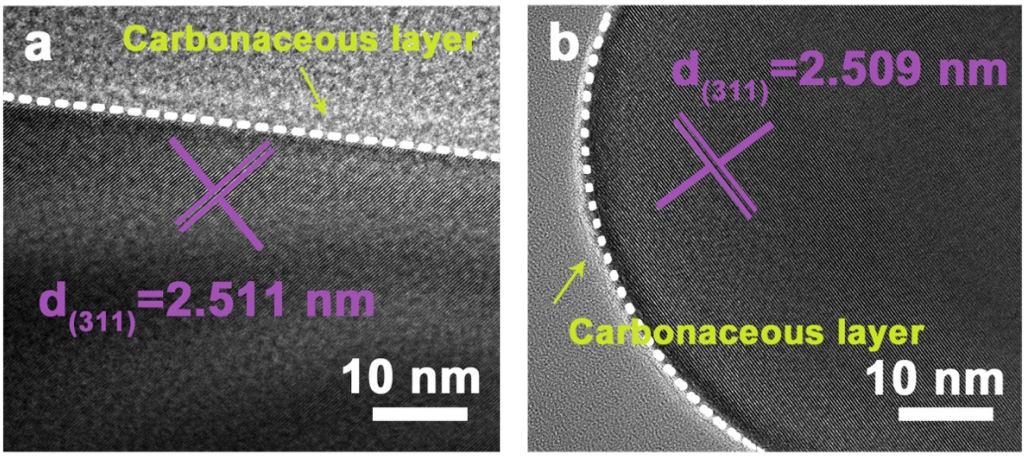

Figure S3. XRD patterns of MESO-X (X=120,140, and 160).

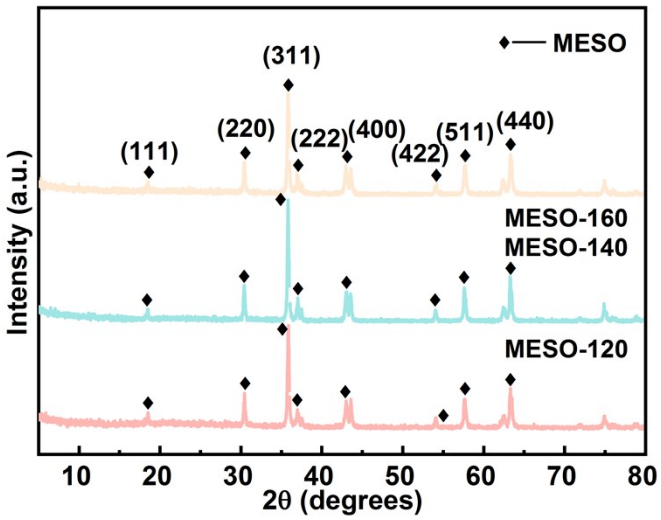

Figure S4. Raman spectra of MESO-X (X=120,140, and 160).

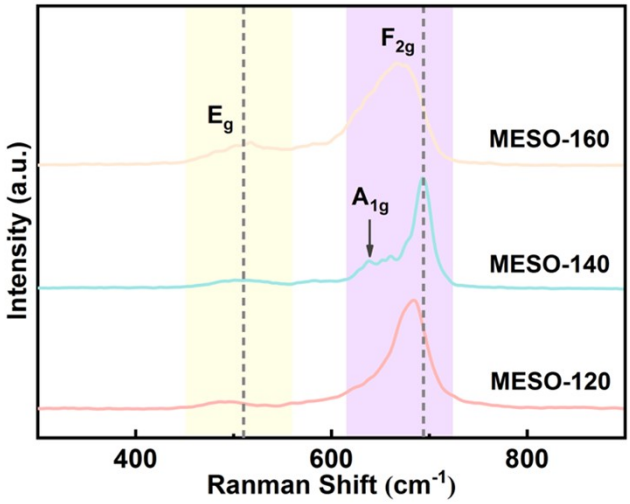

Figure S5. XRD patterns of MESO-X@S (X=120,140, and 160).

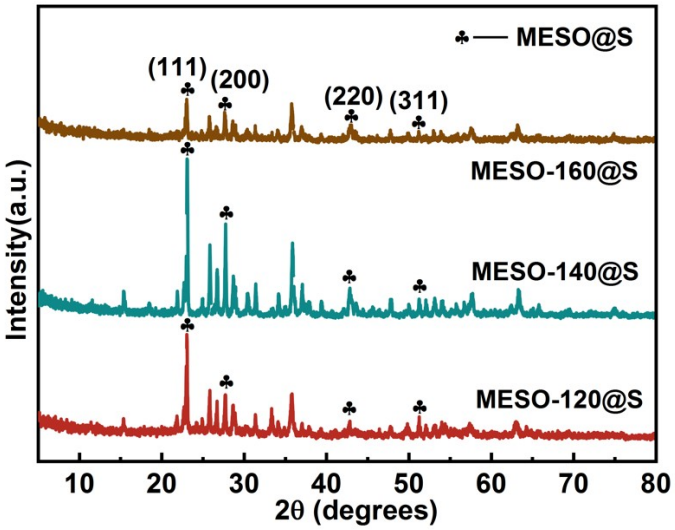

Figure S6. Peak voltage corresponding to the CV profiles of MESO@S.

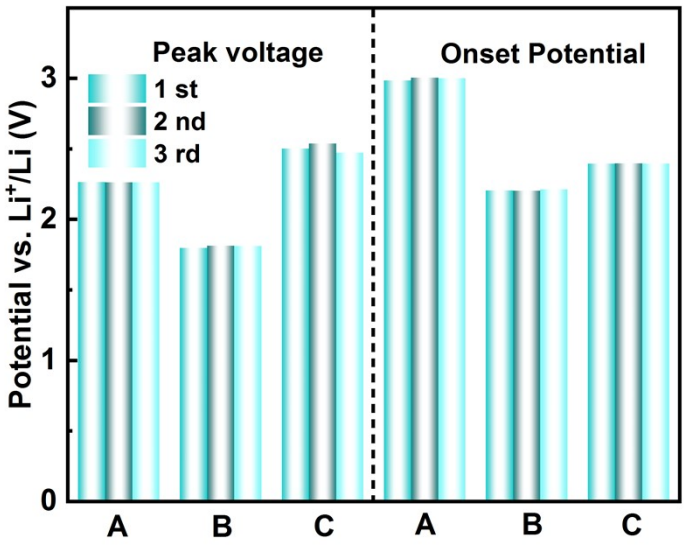

S3. Supporting tables

Table S1. Comparison of the performance of medium-entropy ferrites and oxygen vacancies as cathode materials for Li-S batteries with other published work.

Materials	Cycle number	Current density (C)	Initial special capacity (mAh g^{-1})	Capacity retention (%)	Capacity decay rate (%)	Reference
$CoFe_2O_4$/NC	500	0.2	1096	42	0.076	1
OVs-$MnCo_2O_4$	200	0.5	1089	83.7	0.067	2
HESO/NFs	500	1	656.3	60	0.08	3
ZCo/NCF	300	0.2	1160	77	0.11	4
MCo/NCFs	100	0.2	1177	87	0.13	5
MESO-1C	500	0.1	1309.9	95.6	0.044	This work
OVs-MESO-1C	500	0.1	990.2	89.3	0.107	This work
OVs-MESO-0.1C	100	1	940	33	0.133	This work
MESO-0.1C	100	1	733	48.9	0.097	This work

Supporting references

1 C. Zhang, Y. He, Y. Wang, Y. Liang, A. Majeed, Z. Yang, S. Yao, X. Shen, T. Li and S. Qin, *Applied Surface Science*, 2021, **560**, 149908.

2 H. Wu, R. Xiao, Y. Qiu and H. Wang, *Applied Surface Science*, 2023, **622**, 156939.

3 L. Wu, Y. Hu, Z. Chen, C. Cai, C. Cai, T. Mei, L. Lin and X. Wang, *Electrochimica Acta*, 2022, **432**, 141185.

4 T. Liu, J. Li, H. Cui, Y. Liu, K. Liu, H. Wei and M. Wang, *Journal of Energy Chemistry*, 2023, **76**, 339-348.

5 Y.-Q. Wang, H.-M. Wang, Y.-C. Jiang, G.-R. Li, S. Liu and X.-P. Gao, *ACS Applied Energy Materials*, 2023, **6**, 8377-8387.